Polar-Driven X-ray Backlighter Targets for the National Ignition Facility

Roger Zhang

Webster Schroeder High School

Advisor: **Dr. R. S. Craxton**

Laboratory for Laser Energetics

University of Rochester

Rochester, NY

January 2015

1. Abstract

Imploding x-ray backlighter targets on the National Ignition Facility (NIF) can be used to gather information about primary targets; an initial proposal involves measuring the opacity of materials while they are heated by the NIF laser beams. The backlighter target radiates x rays that are absorbed as they pass through the primary target to a detector. An optimized beam configuration has been developed to maximize the implosion uniformity of the backlighting target (a SiO_2 shell with diameter 2.1 mm and thickness 10 μm) using only the four most polar rings of beams (rings at 23.5° and 30.0° from the poles). Optimization was performed by adjusting parameters such as beam aim points and defocus distances in SAGE, a hydrodynamics simulation code. The uniformity was measured using the rms variation in the center-of-mass radius of the shell, calculated when the target had imploded to approximately half of its original radius. The rms variation was reduced from 26.2% in the initial design to 5.4% in the optimized design. This was achieved primarily by directing 75% of the beams beyond the equator and decreasing their defocus distances to maximize energy deposition near the equator.

2. Introduction

Nuclear fusion has the potential to provide the world with clean, renewable energy. Inertial confinement fusion (ICF) is a method of achieving fusion that involves high power lasers. In ICF, lasers irradiate a plastic or glass shell containing a mixture of deuterium and tritium (DT), causing the shell to ablate outwards and the DT fuel inside to compress. The lasers provide the fuel with enough energy and pressure to fuse together, releasing energy in the process.

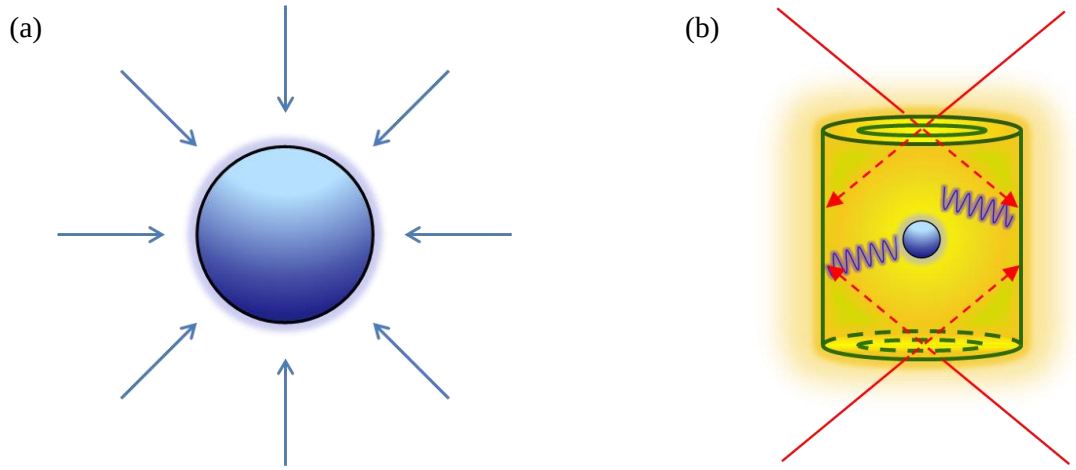

Figure 1: The two main approaches for conducting inertial confinement fusion. (a) In direct drive, beams (represented with arrows) are aimed directly at the target. (b) In indirect drive, beams strike the interior walls of the hohlraum, which emits x rays at the target, compressing it. (Adapted from Fig. 1 of Ref. 5)

There are two primary methods of imploding a target: direct drive[1] and indirect drive,[2] shown in Fig. 1. Direct drive [Fig. 1(a)] involves pointing laser beams directly at the target, thus allowing the laser energy to be used directly in compressing the target. In order to achieve uniform compression using direct drive, the beams must be placed evenly around the target and aimed directly at the center of the target. Indirect drive [Fig. 1(b)] involves placing the target inside a hohlraum, a hollow cylinder typically made of gold with small openings on each of the circular faces. Rather than being pointed directly at the target, the beams are aimed through the

holes at each pole of the hohlraum so that they strike the interior walls. As these walls are struck by the beams, they emit x rays uniformly within the interior of the hohlraum, causing the target inside to heat up and compress. Because indirect drive calls for the beams to enter only through the two holes, a target chamber configured for indirect drive has beam ports positioned around the poles of the target chamber and lacks beam ports surrounding the equator. A disadvantage of indirect drive is that much of the laser energy is absorbed by the hohlraum walls. Only about 20% of the laser energy is absorbed by the target. However, indirect drive does offer the advantage of a more uniform compression.

The National Ignition Facility (NIF) located at the Lawrence Livermore National Laboratory (LLNL) is currently configured for indirect drive; its target chamber has laser beam ports around the poles but not around the equator. The ports are arranged in a total of eight horizontal rings surrounding the target at angles $\theta = 23.5°$, $30.0°$, $44.5°$, and $50.0°$ from the north pole and corresponding angles in the lower hemisphere [Fig. 2]. Beams located on these rings are grouped together in fours (2x2 squares) known as quads. Rings 1, 2, 7, and 8 (the rings closest to the poles) each contain four quads and rings 3, 4, 5, and 6 (the rings closer to the equator) contain eight quads for a total of 48 quads (192 beams).

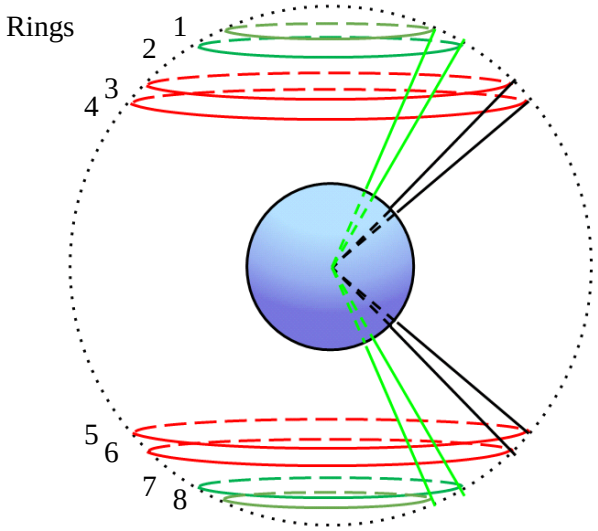

Figure 2: The NIF target chamber. Quads surround the target on rings at 23.5°, 30.0°, 44.5°, and 50.0° from both poles. Rings 1, 2, 7, and 8 each contain four quads and rings 3, 4, 5, and 6 each contain eight quads. Note the lack of beam ports around the equator.

Conducting direct drive experiments with an indirect-drive-configured laser system results in non-uniform implosions. Since beam ports are grouped around the poles, the target's poles are driven with much more energy, causing them to collide long before the equator collapses [Fig. 3(a)]. More uniform direct drive implosions can be achieved on indirect drive-configured lasers by using a technique known as polar drive[3]. In polar drive, beams that were originally aimed at the target's poles are repointed towards the equator, thus compensating for the lack of beam ports surrounding the equator [Fig. 3(b)]. Beam configuration designs optimized to produce more uniform implosions on the NIF based on the concept of polar drive have been developed successfully for DT gas-filled targets.[4]

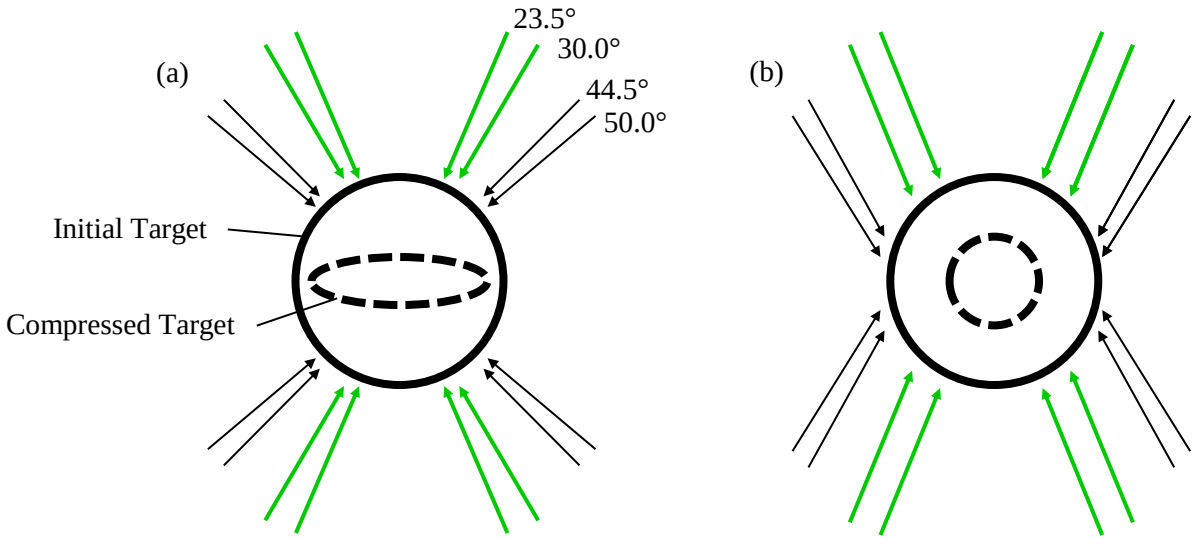

Figure 3: Direct drive on the NIF with and without repointing beams. (a) Keeping the beams pointed directly at the center of the target (as is traditional with direct drive experiments) results in a non-uniform implosion in which the poles of the target collide long before the equator. (b) Repointing the beams allows for more drive near the equator, resulting in a more uniform implosion. (Adapted from Fig. 2 of Ref. 5)

Polar drive can be used to implode other types of targets aside from the usual DT-filled shell. Configurations based on polar drive have been designed to implode D^3He-filled targets for use in proton backlighting.[5] Another useful application of polar drive is x-ray backlighting, when a backlighter target is placed in the target chamber together with a primary target. The backlighter target emits x rays that pass through the primary target and are absorbed by a detector. As the x rays pass through, they can be deflected, absorbed by, or transmitted through the primary target, resulting in an image on the detector. In some experiments the backlighter target needs to be imploded to release x rays, with a certain number of beam ports allocated to the backlighter target and the rest of the beams reserved for the primary target. Such implosion experiments can be useful for testing material properties.

In an initial proposal by Dr. Robert Heeter of LLNL, an x-ray backlighter will be used to measure the opacity of a material when the material is heated up. This primary target (the material) will be mounted onto a half-hohlraum. The beams on the four rings closest to the poles (rings 1, 2, 7, and 8) will be used to implode the x-ray backlighter and the beams on rings 5 and 6 will be aimed into the half-hohlraum to heat up the primary target [Fig. 4]. Since only the four rings of beams closest to the poles are available for the backlighter in this experiment, the beam configuration needed to be optimized to achieve a uniform implosion.

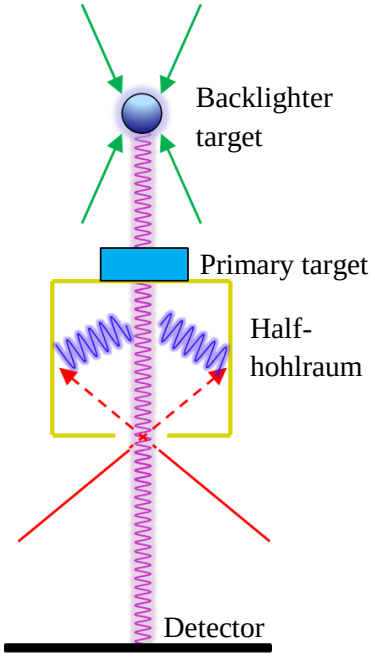

Figure 4: Schematic for the proposed x-ray backlighting experiment. Selected beams are allocated to strike the backlighter target while the others are aimed into the half-hohlraum. The backlighter target implodes, releasing x rays that pass through the primary target and into a detector, creating an image.

3. Simulation Results

The hydrodynamics code *SAGE* was used to simulate target compression with a variety of beam configurations. In these simulations, the backlighter target was a hollow glass shell with an outer diameter of 2100 μm and a thickness of 10 μm. Throughout the optimization process, simulations with different beam configurations were run with the goal of minimizing non-uniformity of the target's center-of-mass radius. The root mean square (rms) deviation percentage was used as the measurement of non-uniformity.

3.1 Initial Design

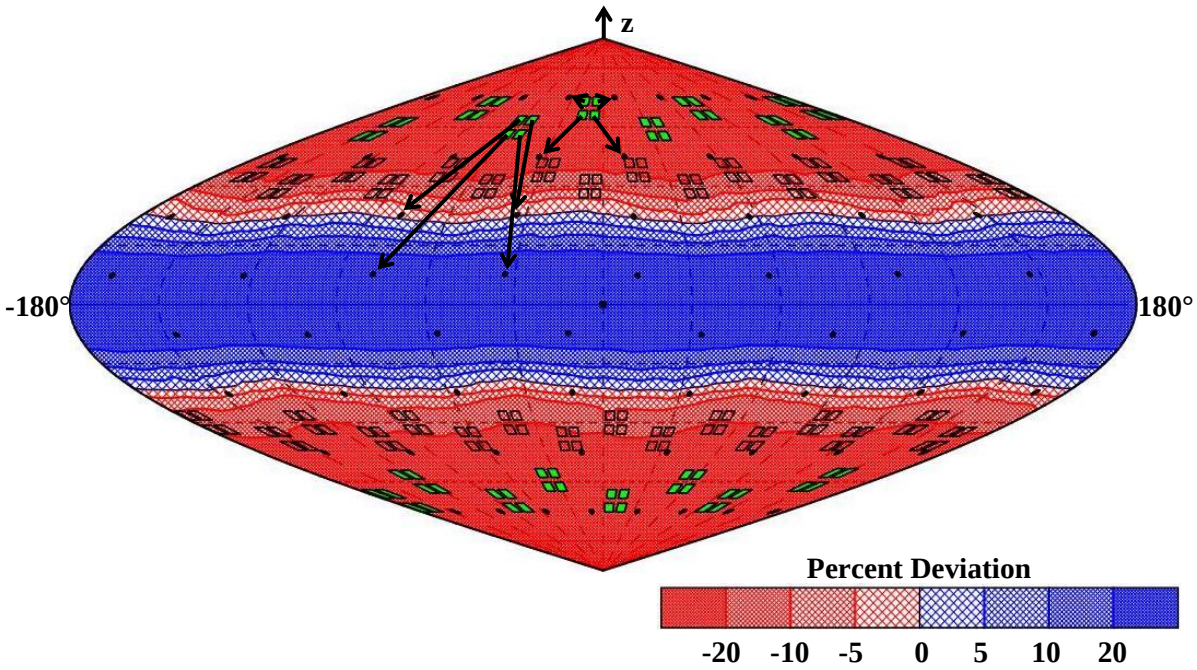

Figure 5: A two-dimensional projection of the target's center-of-mass radius when it has imploded to approximately half of its original radius using the initial design. Shades of red and blue indicate the percent deviation from the average center-of-mass radius of the target. The groups of four squares (2x2) represent the locations of the quads in the target chamber. Quads colored green are used to implode the backlighter while clear quads are used for the primary target (or turned off). Black points show the beam aim points. Examples of quads and their aim points on rings 1 and 2 are shown with arrows. The rms deviation was 26.2% for this initial design.

Figure 5 is a two-dimensional projection of the target's center-of-mass radius when it has imploded to approximately half of its original radius using the initial design. The contours and shading show the percent variation of the target's center-of-mass radius. In the initial design, beam aim points (shown by black points) were positioned at angles of 20°, 40°, 60°, and 80° from each pole, and were spread evenly across in the horizontal direction. This resulted in a very uneven compression. As shown by the dark blue shading around the equator and the dark red shading near the poles, the target's poles were compressed far more than the equator. The target's center-of-mass radius over the entire surface had an rms variation value of 26.2%. The first step in improving this design was to increase energy deposition around the equator.

The process of minimizing the rms variation of the target's surface was carried out through changing the beam aim points and defocus distances. The defocus distance is the distance between the laser beam's best focus and the target (if the defocus distance is zero, the beam will be at best focus on the target). Increasing the defocus distance results in an increased beam spot size on the target's surface; this spreads out the laser energy over a greater surface area. Decreasing it results in a smaller beam spot size.

3.2 Improved Design

Due to the nature of polar drive, beams shifted towards the equator don't strike the target at normal incidence. Since these beams are oblique, less energy is deposited, resulting in a need to direct more beam energy towards the equator. To counteract the reduced energy absorption near the equator, beam aim points for 75% of the beams were shifted beyond the equator (see Fig. 6). In addition, the defocus distances of these beams were decreased, resulting in smaller but more focused beam spots on the target. The beam aim points for the other 25% of beams (the upper beams on the 23.5° ring) were positioned on rings at only 25° from the poles. Since these beams strike the target at a much less slanted angle, there is greater energy deposition in the region near the poles. It was found that sufficient energy deposition could be achieved near the poles by using these beams and that uniformity could be improved by increasing the defocus distances of these beams.

As seen in Fig. 6, the equator no longer shows dark blue shading as it did in Fig. 5, indicating success in increasing the drive near the equator and resulting in a much more uniform implosion. The rms variation of the target's center-of-mass radius using the improved design was 5.7%, significantly less than the original 26.2%.

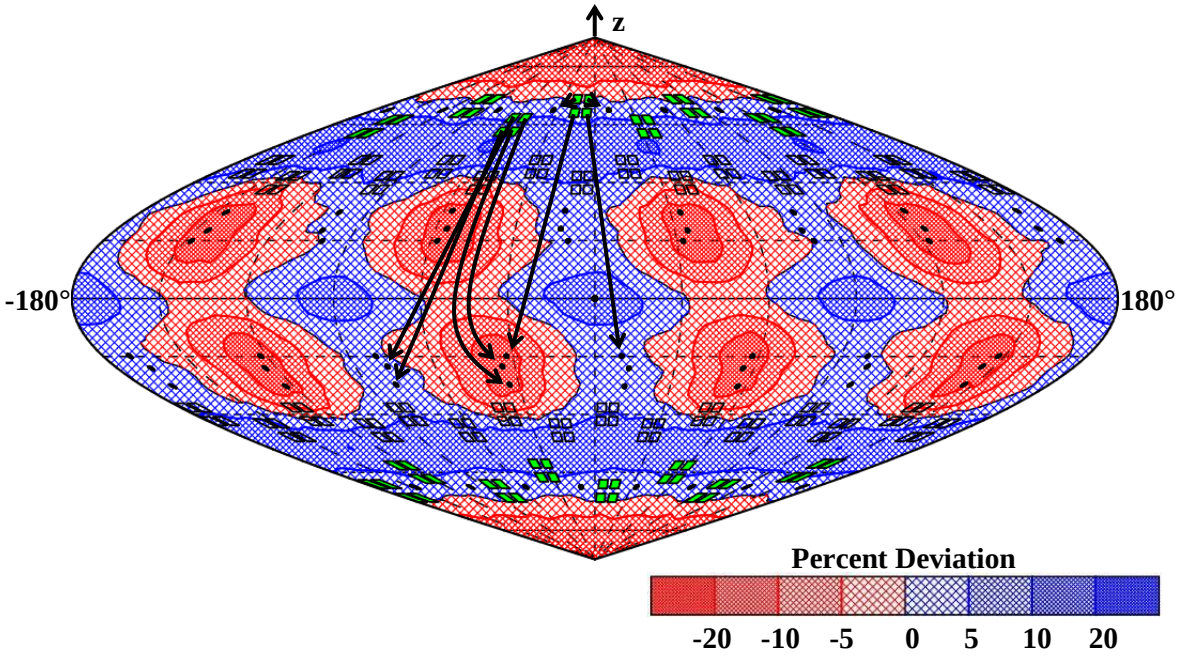

Figure 6: Same as Figure 5 except for the improved design. In this design, all but the very top (and very bottom) rows of beams are aimed beyond the equator in an effort to increase the drive at the equator. The rms deviation for this improved design was 5.7%.

Figure 7 shows the shifts of the beam aim points more clearly. In the improved design [Fig. 7(b)], beams that were originally aimed near the poles in the initial design [Fig. 7(a)] were repointed towards the equator. The slight decrease in defocus distance can also be seen; each of the two beams shown is slightly narrower in the improved design.

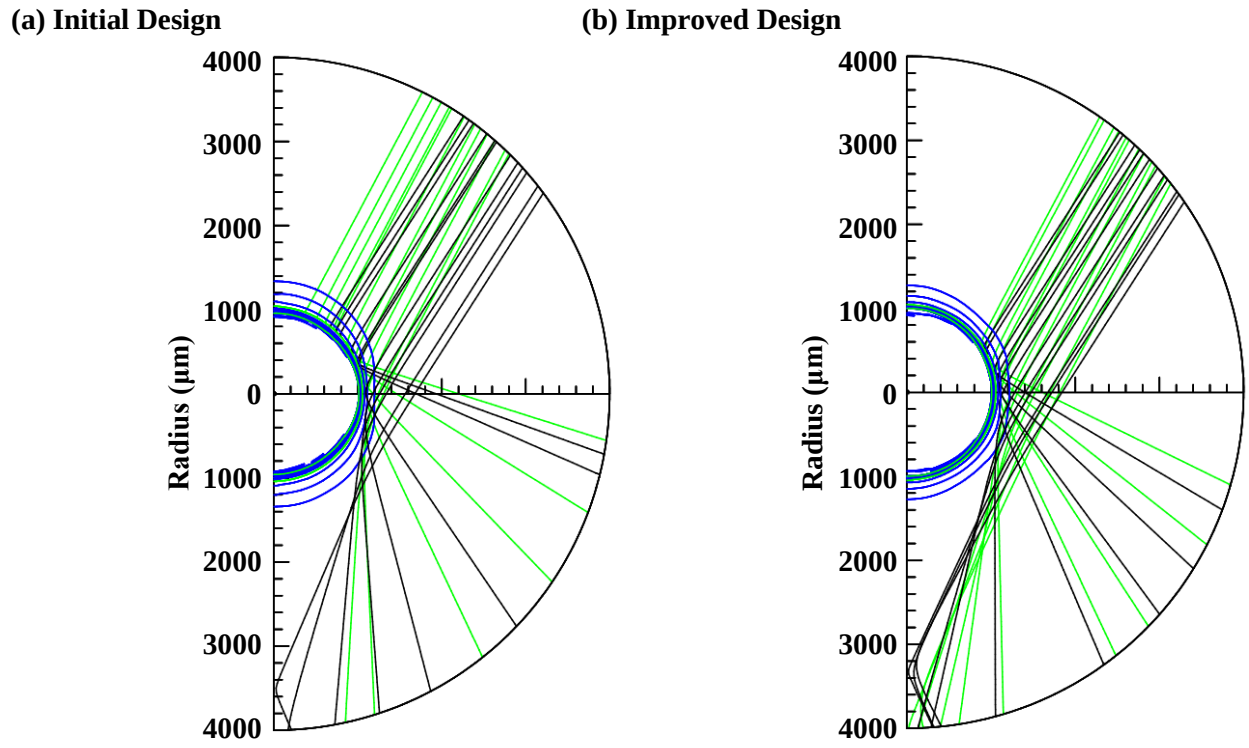

Figure 7: Raytrace plots of two beams (colored green and black) very early on in the simulation (1000 ps). The target's shell is shown in blue. (a) In the initial design, not enough beams are aimed towards the equator, resulting in low compression near the equator. (b) In the improved design, a greater number of beams are aimed near the equator to increase the drive there.

Even with the significant improvement with this design, however, there were still a few problems. As shown in Fig. 6, there existed horizontal regions just below the poles with too little energy. Furthermore, areas of above average compression near the equator (shown by the red circles) on the upper hemisphere lined up with those on the lower hemisphere.

3.3 Optimized Design

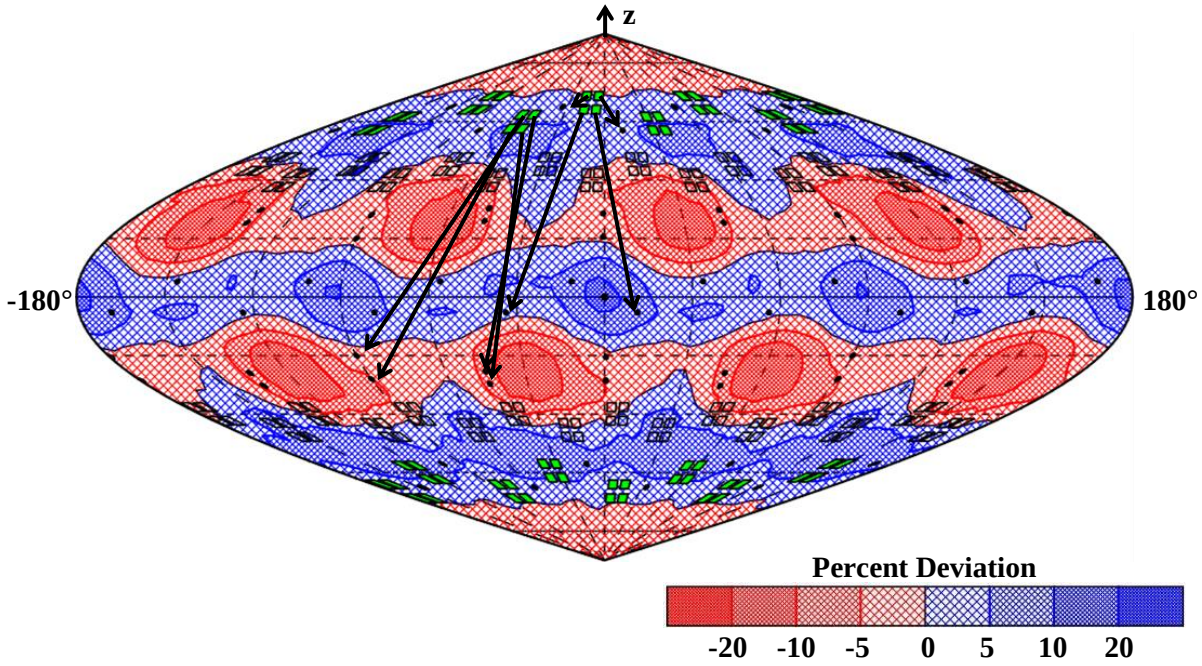

Figure 8: Same as Figure 6 except now using the optimized design. The rms deviation for this optimized design was 5.4%.

Figure 8 is a projection of the target's center-of-mass radius deviation using an optimized beam configuration. The optimized design resolves some of the issues with the previous design. The aim points for the beams aimed towards the poles have been altered slightly and the remaining beams have been shifted in the horizontal (ϕ) direction to reduce overlapping of the high energy spots. The rms non-uniformity for this optimized design was 5.4%, slightly below the previous design's 5.7% and much lower than the initial design's 26.2%.

The target's center-of-mass radius as a function of θ (averaged over ϕ), measured when the target has imploded to approximately half of its original radius, is shown in Fig. 9 (blue) for the initial design. The poles ($\theta = 0°$ and 180°) received too much energy, resulting in a quick compression of the poles while the equator ($\theta = 90°$) received little energy, resulting in a very slow compression near the equator. Using the optimized design, the target's center-of-mass

radius (green), while still exhibiting some degree of variation, is much more even during the implosion.

Table 1 shows the beam aim points and defocus distances used in the optimized design.

Ring	Port Position	θ (deg.)	Δϕ (deg.)	Defocus (cm)	Ring	Port Position	θ (deg.)	Δϕ (deg.)	Defocus (cm)
1 (23.5°)	T, L	25.00	-22.5	3.0	7 (156.5°)	T, L	60.00	-11.25	1.0
	T, R	33.00	22.5	3.0		T, R	61.67	33.75	1.0
	B, L	95.33	-22.5	1.0		B, L	64.30	-11.25	1.0
	B, R	95.33	22.5	1.0		B, R	69.71	33.75	1.0
2 (30.0°)	T, L	110.26	-33.75	1.0	8 (150.0°)	T, L	84.67	-22.5	1.0
	T, R	115.69	11.25	1.0		T, R	84.67	22.5	1.0
	B, L	118.30	-33.75	1.0		B, L	147.0	-22.5	3.0
	B, R	120.00	11.25	1.0		B, R	155.0	22.5	3.0

Table 1: Beam aim points and defocus distances used in the optimized design. All quads on the same ring are configured identically with the same θ and Δϕ (horizontal shift) values, and the same defocus distances. The ports within each quad are denoted by T (top) or B (bottom), and L (left) or R (right). For example, (T, L) would indicate the top left port of a quad.

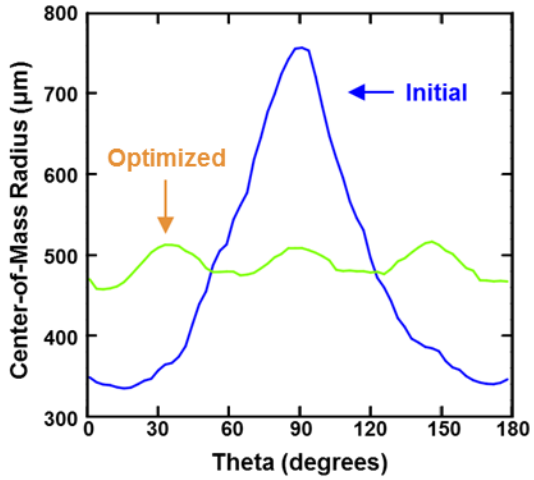

Figure 9: A comparison of the target's center-of-mass radius during implosion using the initial design (blue) and the optimized design (green). The poles lie at 0° and 180° and the equator at 90°.

The laser pulse profile was changed for the optimized design from that used for the initial and improved designs to reduce the maximum power and energy. The laser pulse for both the initial and improved designs (Fig. 10) called for a total power of 220 TW to be used for the backlighter. However, because only one third of the NIF's beams are being used for this backlighter (beams on rings 1, 2, 7, and 8), the equivalent total power output would be three times as much, 660 TW, in excess of the 400 TW limit that is usually imposed. A revised laser pulse shape was used for the

optimized design. Figure 10 shows how the peak power was reduced to 133 TW, decreasing the energy needed for the backlighter from 350 kJ to only 260 kJ. The equivalent total energy was decreased from 1050 kJ to 780 kJ. While the NIF is designed for a maximum energy of 1.8 MJ, it is preferred to operate below 800 kJ to minimize damage to the laser system.

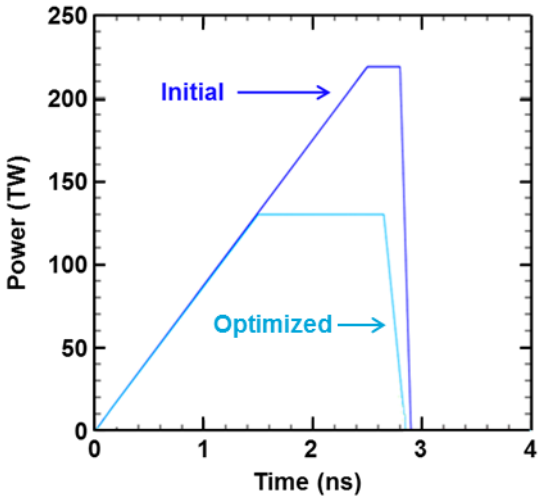

Figure 10: A comparison of the pulse shape used for the initial and improved designs (dark blue) to the pulse shape used for the optimized design (light blue).

4. Future Applications

As discussed previously, there is an initial proposal to use this optimized design to backlight a heated material to measure its opacity. However, x-ray backlighting can be used to image several other types of targets such as a polar-driven target or a hohlraum.

5. Conclusion

A design has been developed to provide an implosion source for x-ray backlighting on the NIF using only the beams from the four rings closest to the poles. Optimization of the beam configuration to increase the uniformity of the implosion was performed using the hydrodynamics simulation code *SAGE*. The rms non-uniformity of the target's center-of-mass radius during implosion was reduced from 26.2% to 5.4%.

6. Acknowledgements

I would like to thank Dr. Stephen Craxton for providing me with this unique research opportunity and for his advice and support throughout the project. I would also like to thank the Laboratory for Laser Energetics for running the high school summer research program.

References

[1]J. Nuckolls, L. Wood, A. Thiessen, and G. Zimmerman, "Laser compression of matter to super-high densities: Thermonuclear (CTR) applications," Nature **239**, 139 (1972).

[2]J. D. Lindl, *Inertial Confinement Fusion: The Quest for Ignition and Energy Gain Using Indirect Drive* (Springer-Verlag, New York, 1998).

[3]S. Skupsky, J. A. Marozas, R. S. Craxton, R. Betti, T. J. B. Collins, J. A. Delettrez, V. N. Goncharov, P. W. McKenty, P. B. Radha, T. R. Boehly, J. P. Knauer, F. J. Marshall, D. R. Harding, J. D. Kilkenny, D. D. Meyerhofer, T. C. Sangster, and R. L. McCrory, "Polar direct drive on the National Ignition Facility," Phys. Plasmas **11**, 2763 (2004).

[4]A. M. Cok, R. S. Craxton, and P. W. McKenty, "Polar-drive designs for optimizing neutron yields on the National Ignition Facility," Phys. Plasmas **15**, 082705 (2008).

[5]Y. Kong, "Beam-Pointing Optimization for Proton Backlighting on the NIF," Laboratory for Laser Energetics High School Summer Research Program (2013).